

## Evi3, a zinc-finger protein related to EBF<sub>1</sub>, regulates EBF activity in B-cell leukemia

Kathryn E Hentges<sup>1,4</sup>, Keith C Weiser<sup>1,2</sup>, Tony Schountz<sup>1,5</sup>, Lanette S Woodward<sup>1</sup>, Herbert C Morse III<sup>3</sup> and Monica J Justice<sup>\*1</sup>

<sup>1</sup>Department of Molecular and Human Genetics, Baylor College of Medicine, One Baylor Plaza, Houston, TX 77030, USA;

<sup>2</sup>Interdepartmental Program in Cell and Molecular Biology, Baylor College of Medicine, Houston, TX 77030, USA; <sup>3</sup>Laboratory of Immunopathology, National Institute of Allergy and Infectious Diseases, National Institutes of Health, Rockville, MD, USA

**Retroviral insertions that activate proto-oncogenes are a primary cause of tumors in certain strains of mice. The AKXD recombinant inbred mice are predisposed to a variety of leukemias and lymphomas as a result of viral integration. One common insertion site, the ecotropic viral insertion site 3 (Evi3), has been implicated in most B-cell tumors in the AKXD-27 strain. The Evi3 gene encodes a zinc-finger protein with sequence similarity to the Early B-cell Factor-Associated Zinc-finger gene (EBFAZ). We show that the Evi3 gene is overexpressed in several tumors with viral insertions at Evi3, which results in the upregulation of Early B-cell Factor (EBF)-target gene expression, suggesting that Evi3 modulates EBF activity. Reconstitution of primary leukemia cells showed that these tumors express high densities of the B-cell surface proteins CD19 and CD38, which are EBF targets. Using a transactivation assay, we show that the terminal six zinc-fingers of Evi3 are required for modification of EBF activity. This is the first evidence that Evi3 expression in tumors alters the level of EBF target genes, and the first characterization of the Evi3 protein domains required for modulation of EBF activity. Further, these data imply that Evi3 misexpression initiates tumorigenesis by perturbing B-cell development via an interaction with EBF.**

*Oncogene* (2005) 24, 1220–1230. doi:10.1038/sj.onc.1208243  
Published online 6 December 2004

**Keywords:** *Evi3*; *EBF*; Pax-5; mb-1; B29; B-cell leukemia

### Introduction

The AKXD recombinant inbred strains of mice are a valuable system for the study of the molecular genetic basis for the development of leukemia and lymphoma

(Mucenski *et al.*, 1986, 1987, 1988; Gilbert *et al.*, 1993). These mice develop a variety of B-cell and T-cell lymphomas and leukemias due to somatic proviral insertions that alter gene expression of proto-oncogenes or tumor suppressor genes. The integrated provirus can serve as a tag to clone novel genes involved in the leukemia or lymphoma disease process. The AKXD mouse strains are valuable for identifying new genes that lead to the development of B-lineage tumors (Mucenski *et al.*, 1987; Justice *et al.*, 1994; Hansen *et al.*, 2000; Suzuki *et al.*, 2002).

If independent tumors from different mice have proviral insertions at the same genomic site, then it is likely that the region flanking the insertion contains a proto-oncogene. Thus, the identification of common sites of viral insertion is likely to identify genes responsible for oncogenesis. One common proviral insertion site identified from AKXD B-cell tumors is the ecotropic viral insertion site 3 (*Evi3*) (Justice *et al.*, 1994). In the AKXD-27 recombinant inbred strain of mice, 70% (seven of 10) of pre-B and B-cell tumors contained proviral insertions at *Evi3*, whereas no T-cell or myeloid tumors contained insertions, indicating that insertions at *Evi3* cause tumors of the B-cell lineage (Justice *et al.*, 1994).

*Evi3* is located on proximal mouse chromosome 18 in a region of homology to human chromosome 18q12 (Justice *et al.*, 1994). Cloning of mouse genomic DNA revealed that *Evi3* lies within a CpG island, indicating that the proviral insertions were likely near the promoter or 5' end of a gene (Justice *et al.*, 1994). Northern blots with the *Evi3* insertion site genomic probe identified transcripts that are expressed in developing B-cells, but not mature B-cells, suggesting that the gene encoded at *Evi3* may play a role in B-cell differentiation or survival (Justice *et al.*, 1994).

The gene encoded at *Evi3* is a novel multiple zinc-finger-containing protein (Warming *et al.*, 2003) with similarity to Early B-cell Factor-Associated Zinc-finger (*EBFAZ/ROAZ/OAZ*) (Tsai and Reed, 1998; Hata *et al.*, 2000). *EBFAZ* has been demonstrated to modulate the transcriptional activation activity of Olf-1/EBF, a helix–loop–helix transcription factor identified as a regulator of both B-cell development and olfactory neuron differentiation (Tsai and Reed, 1997; Wang *et al.*,

\*Correspondence: MJ Justice, Department of Molecular and Human Genetics, Baylor College of Medicine, Room S413, One Baylor Plaza, Houston, TX 77030, USA; E-mail: mjustice@bcm.tmc.edu

<sup>4</sup>Current address: Faculty of Life Sciences, University of Manchester, Manchester, M13 9PT, UK.

<sup>5</sup>Current address: Department of Biology, Mesa State College, Grand Junction, CO 81506, USA.

Received 17 November 2003; revised 4 October 2004; accepted 5 October 2004; published online 6 December 2004

1997). Here, we analyse the expression of *Evi3*, as well as a number of Early B-cell Factor (EBF) target genes in tumors with proviral insertions at *Evi3*. We also determine the immunophenotype of reconstituted primary tumor cells to show that EBF target genes are highly expressed on the surface of tumor cells with *Evi3* insertions. Together, our data suggest that activation of EBF target genes leads to leukemia. Further investigation of the role of *Evi3* during normal B-cell development and in B-cell tumors will provide clues as to how this gene functions during oncogenesis.

## Results

### *Tumors that arise in the AKXD-27 strain*

To obtain additional primary tumor samples with retroviral insertions at *Evi3*, we aged mice from the AKXD-27 strain, a strain that had previously shown a high predominance of tumors with insertions at *Evi3*. Previous studies of lymphoma susceptibility in AKXD mice evaluated only females. To address the possibility of differences in male versus female lymphoma susceptibility, approximately equal numbers of male and female mice were aged. In all, 31 of 40 female mice (77.5%) developed tumors, whereas 10 of 34 male mice (29%) developed tumors. This number is significantly different from the expected value ( $\chi^2$ ;  $P < 0.05$ ), and suggests a sex bias towards tumor development in AKXD-27 female mice. This sex-specific bias was not observed in other AKXD strains (data not shown).

Tumors that arise in AKXD-27 mice were classified by antigen receptor rearrangements and histopathology (Table 1). We found a diverse array of lymphoid tumors based upon BCR (IgH and/or Ig $\kappa$ ) and TCR (J $\beta$ 1 or J $\beta$ 2) rearrangements. We classified tumors with IgH, but not Ig $\kappa$  rearrangements as pro-B-cell tumors, and those with rearrangements of IgH and Ig $\kappa$  as pre-B-cell tumors (Mucenski *et al.*, 1988). Of the B lineage tumors identified, only three had rearrangements at the Ig $\kappa$  locus, suggesting that most of these immature B-lineage tumors arise in the bone marrow. In the present study, B-cell lineage tumors were found in 70% of the total tumors examined. Eight tumors harbored retroviral insertions at *Evi3*, an insertion site that has been frequently observed in AKXD-27 B-cell tumors (Justice *et al.*, 1994). Seven of these were classified as pro-B-cell tumors, whereas one tumor had no TCR or BCR rearrangements, and is classified as a progenitor tumor by histopathology (H Morse, personal communication). All *Evi3* proviral insertions occurred in female mice.

### *Analysis of the Evi3 gene*

We identified and sequenced two IMAGE clones (www.image.llnl.gov, #5359310 and #5038671) that contained *Evi3* transcript sequence. Analysis of the two sequences revealed that the IMAGE clone #5359310 (Genbank #BI730849) insert contains a longer 3'UTR,

but the same predicted open reading frame as IMAGE clone #5038671 (Genbank #BC021376). The IMAGE clone #5359310 complete insert sequence is 6033 bp, compared with 4781 bp for IMAGE clone #5038671. The *Evi3* gene cDNA sequence identified by Warming *et al.* (2003), Genbank #AY147406, also lacks the longer 3'UTR identified from our sequencing of the IMAGE clone #5359310.

The proviral insertions at *Evi3* have been localized to the first intron of the *Evi3* gene (Figure 1a). Interestingly, the viral insertions in six of the *Evi3* tumors from the re-aged AKXD-27 strain cluster in a stretch of only 22 bp directly upstream of the initiation codon of the *Evi3* gene (Figure 1b), in a similar location as the viral insertions in *Evi3* tumors identified by Warming *et al.* (2003). Insertions at *Evi3* in the initial tumors clustered within a 200 bp region as determined by Southern blot data (Justice *et al.*, 1994), suggesting that viral insertions in a small region are required to disrupt the normal expression of the *Evi3* gene to cause leukemia.

The *Evi3* transcript is encoded by eight exons and spans approximately 286 kb of genomic DNA. It shows 88% sequence similarity to *EBFAZ* (Tsai and Reed, 1997), which is located on mouse chromosome 8. The *Evi3* predicted protein is 1312 amino acids, contains 30 Krüppel family zinc-fingers (Figure 1c), and shares 63% homology to the *EBFAZ* predicted protein. Based on the protein sequence similarity to *EBFAZ*, we examined the possibility that *Evi3* could be involved in B-cell differentiation through regulation of EBF activity.

### *Expression analysis of the Evi3 gene*

*Evi3* expression levels were examined in wild-type tissues, B-cell lines, and tumors from AKXD-27 animals with or without viral insertions at *Evi3*. Quantitative real-time PCR was used to optimize the expression analysis from RNAs made from tumor tissues. *Evi3* expression has been observed in wild-type B-cells at all stages from Pro-B to mature B-cells (Warming *et al.*, 2003). To evaluate relative expression levels through quantitative real-time PCR, we selected one tissue sample, wild-type spleen, as our standard. Expression levels in other tissues are shown as fold changes relative to the expression level in spleen, which was designated as one. The results are shown on a logarithmic scale (Figure 2a). We used wild-type spleen as our standard, since in most cases spleen was used to isolate tumor RNA. In wild-type tissues, *Evi3* was highly expressed in adult brain, 12.5 dpc embryos, adult lung, testes, and B220+ cells as compared to spleen (Figure 2a). The NFS-467 cell line, which has a viral insertion at *Evi3* (Justice *et al.*, 1994), also had higher levels of *Evi3* expression relative to wild-type spleen (Figure 2a).

We then examined *Evi3* expression levels in B-cell tumors with viral insertions at *Evi3* as compared to B-cell tumors without insertions in the *Evi3* locus (Figure 2b and c). All tumors were from female mice. For these studies, we compared the expression levels to tumor C27-193, a Pro-B tumor without an *Evi3*

**Table 1** Molecular and histopathological characteristics of AKXD-27 tumors

Mouse	Sex	TCR <sub>Jβ1</sub>	TCR <sub>Jβ2</sub>	IgH	Igκ	Evi3	Emv	Mcf	Histopathology <sup>a</sup>	Classification <sup>b</sup>
27-1	F	+	-	+	-	-	+	+	LL	Mixed T/B
27-3	F	-	-	+	+	-	+	-	LL	Pre-B
27-10	F	-	-	-	-	-	-	-	EMZ	B-cell <sup>c</sup>
27-11	F	-	-	+	-	-	-	+	LL	Pro-B
27-12	F	-	-	+	-	-	+	+	LL	Pro-B
27-13	F	+	-	-	-	-	-	+	LL	T
27-16	F	-	-	+	-	+	+	-	LL	Pro-B
27-17	F	-	-	-	-	-	-	-	LL	Unclassified
27-24	F	+	-	-	-	-	+	+	FL/MZL	T
27-28	F	-	-	+	-	-	+	-	LL	Pro-B
27-30	F	-	-	-	+	-	-	+	HS/MZL	Pre-B
27-35	M	+	-	+	-	-	+	-	CB/FL	Mixed T/B
27-47	M	-	-	+	-	-	+	+	LL	Pro-B
27-57	F	-	-	+	-	+	+	+	CB/FL	Pro-B
27-73	M	+	-	-	-	-	ND	ND	LL	T
27-77	M	-	-	+	-	-	ND	ND	LL	Pro-B
27-84	F	-	+	-	-	-	ND	ND	LL	T
27-94	M	+	-	-	-	-	ND	ND	LL	T
27-107	M	-	-	-	-	-	+	+	LL	Unclassified
27-110	F	-	+	-	-	-	+	+	LL	CD4 <sup>+</sup> T <sup>d</sup>
27-128	F	-	-	+	-	-	-	-	LL	Pro-B
27-129	F	-	-	-	-	-	+	+	LL	Progenitor
27-142	M	-	+	+	-	-	+	+	LL	Mixed T/B
27-165	F	+	+	+	-	-	+	+	LL	Mixed T/B
27-172	F	-	-	+	-	+	+	+	LL	Pro-B
27-178	M	-	-	+	-	-	-	+	LL	Pro-B
27-183	F	-	-	+	-	+	+	+	LL/MZL	Pro-B
27-184	F	-	-	+	-	-	+	+	LL	Pro-B
27-186	M	+	+	+	-	-	-	+	LL	Mixed T/B
27-189	F	-	-	+	-	-	-	+	IBL	Pro-B
27-193	F	-	-	+	-	-	-	+	LL	Pro-B
27-205	F	-	-	+	-	+	+	+	LL	Pro-B
27-207	F	-	-	-	-	+	+	+	LL	T lymphoblast <sup>e</sup>
27-215	F	+	+	-	-	-	+	+	LL	T
27-222	F	-	-	+	-	+	+	+	MML	Pro-B
27-224	F	+	+	+	-	-	+	+	LL	Mixed T/B
27-242	M	+	+	-	-	-	+	+	LL	T
27-258	F	-	-	+	-	+	+	+	LL/MZL	Pro-B
27-266	F	-	-	+	+	-	+	+	LL	Pre-B
27-268	F	+	+	+	-	-	+	+	LL	Mixed T/B
27-316	F	+	-	+	-	-	-	+	LL	Mixed T/B

Genomic DNA was extracted from AKXD-27 mice (*n* = 41) with lymphoid tumors and probed by Southern blot analysis for antigen receptor rearrangements or viral insertion mutations at *Evi3*. Tumors were classified based upon molecular rearrangements of receptor genes. <sup>a</sup>Histopathology designations: LL – lymphoblastic leukemia, MZL – marginal zone lymphoma, FL – follicular B-cell lymphoma, CB – centroblastic lymphoma, HS – histocytic sarcoma, EMZ – enlarged marginal zone, MML – myelomonocytic leukemia, IBL – immunoblastic lymphoma. <sup>b</sup>IgH rearrangements indicate pro-B lymphoma; Igκ rearrangements indicate pre-B lymphoma; TCR-Jβ rearrangements indicate T-cell lymphoma; both BCR and TCR rearrangements indicated mixed lymphoma. <sup>c</sup>Tumor cells expressed CD117 (*c-kit*) by flow cytometry. <sup>d</sup>Tumor cells were CD4<sup>+</sup>/CD8<sup>-</sup> by two-color flow cytometry. <sup>e</sup>Tumor classification based on pathology. Emv = Ecotropic murine leukemia virus. Mcf = Mink cell focus forming virus

insertion. We chose this sample as our standard because it is the same stage as most of the *Evi3* tumors, and because it is a spleen tumor with cellularity similar to the *Evi3* tumors examined. In AKXD-27 tumors with insertions at *Evi3*, expression levels of *Evi3* ranged from fourfold higher than control tumor C27-193 up to 217 times the expression level in the control tumor, with all *Evi3* tumors except 27-258 showing higher expression than the control tumors. In AKXD-27 tumors without *Evi3* insertions, only one tumor showed slightly elevated levels of *Evi3* as compared to the control tumor C27-193 (C27-224, Figure 2c). When the expression levels of *Evi3* in the tumors with viral insertions at *Evi3* are compared to the tumors without insertions, there is a dramatic

upregulation of *Evi3* in the tumors with viral insertions (Figure 2b and c).

The *Evi3* predicted protein shows homology to EBFAZ, a protein that interacts with EBF and negatively regulates EBF target gene transcription in the olfactory epithelium (Tsai and Reed, 1997). To determine if *Evi3* expression could modulate EBF activity, we examined the expression of *EBF* and *EBF*-target genes in tumors from AKXD-27 mice with or without viral insertions at *Evi3*. We found that *EBF* was expressed in tumors with viral insertions at the *Evi3* locus (Figure 2b). The expression levels of *EBF* are elevated 40–185 times over levels in non-*Evi3* tumor C27-193. *EBF* levels in control tumors without *Evi3*

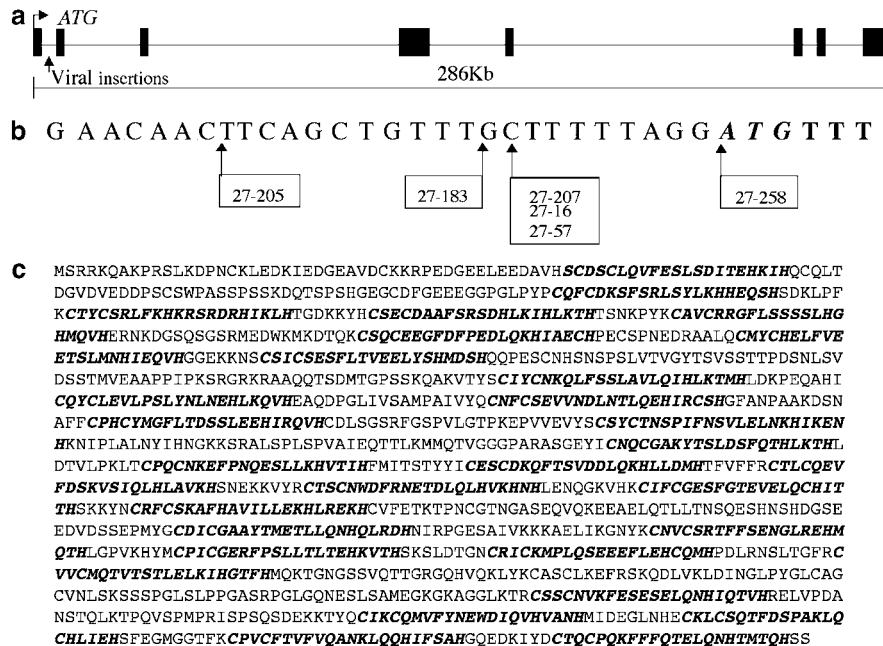


**Figure 1** Genomic structure and protein sequence of the *Evi3* gene. Panel a: The *Evi3* gene is comprised of eight exons. Viral insertions are found in intron 1 (arrow), just upstream of the start codon (ATG). Panel b: Viral insertion sites in the tumors are clustered within 22 bp upstream of the initiation codon of the *Evi3* gene, shown in bold italics. Panel c: The *Evi3* predicted protein contains 30 zinc-fingers, shown in bold italics

insertions are only 1–2-fold higher than control C27-193 (Figure 2c), with most tumors showing no increase in *EBF* expression, suggesting that *EBF* positively regulates its own expression. The *EBF* promoter has been demonstrated to contain *EBF*-binding sites, and co-transfections of *EBF* and an *EBF* promoter reporter construct in HeLa cells demonstrated that *EBF* can induce its own expression (Smith et al., 2002). Our study extends this finding to leukemia samples.

To further examine the effect of *Evi3* overexpression in AKXD-27 tumors, we analysed the expression levels of *EBF*-target genes in tumors with the *Evi3* insertion and compared the levels to tumors without the *Evi3* insertion. *EBF* has been demonstrated to directly regulate the transcription of *mb-1* and *B29*, components of the pre-B-cell receptor (Hagman et al., 1993; Akerblad et al., 1999; Gisler et al., 2000). The expression of *mb-1* in *Evi3* tumors (Figure 2b) is elevated as compared to non-*Evi3* tumors (Figure 2c), with levels ranging from 208 to 1822 times increased expression as compared to C27-193. In non-*Evi3* tumors, four tumors show an increase in *mb-1* expression as compared to C27-193. However, only one control, C27-189, shows an increase in the same range as some of the *Evi3* tumors. Likewise, the expression levels of *B29* are greatly increased in *Evi3* tumors (Figure 2b) as compared to tumors without insertions at *Evi3* (Figure 2c). All *Evi3* tumors show increased expression compared to C27-193. One non-*Evi3* tumor, C27-189, shows an increase in the same range as the *Evi3* tumors, but four non-*Evi3* tumors have lower levels of *B29* relative to C27-193. In contrast to results shown in the olfactory epithelium (Tsai and Reed, 1997), our results indicate that *EBF*

target genes are activated as a result of the virally induced overexpression of *Evi3*.

The expression levels of *Pax-5* (also called B-cell-specific activator protein (*BSAP*)), another direct target of *EBF* (O’Riordan and Grosschedl, 1999), were analysed in *Evi3* and control tumors. All *Evi3* tumors show expression levels that are increased as compared to tumor C27-193, with values ranging from 100-fold to more than 1000-fold greater expression (Figure 2b). All the control tumors have expression that is increased relative to C27-193, but the expression increase ranges from only slightly more than two times to 100 times the C27-193 level (Figure 2c).

All of the *Evi3* tumors show higher expression of *EBF*-target genes than control tumors, with the exception of control tumors C27-189 and C27-266, which have similar levels of *mb-1* and *Pax-5* as the *Evi3* tumors 27-207 and 27-183. However, the majority of the *Evi3* tumors show upregulation of the target genes as compared to control tumors. For most of the target genes, the control tumors have expression in the range of two to 10 times the C27-193 level, while the *Evi3* tumors show expression levels greater than 10–1000 times the expression levels of tumor C27-193. These results suggest that upregulation of *Evi3* expression leads to increased transcription of *EBF* target genes through modulation of *EBF* activity.

#### Flow cytometry on *Evi3* tumors

To determine the immunophenotype of tumor cells mis-expressing *Evi3*, we reconstituted tumors by injecting cryopreserved cells from the leukemic spleen of mouse

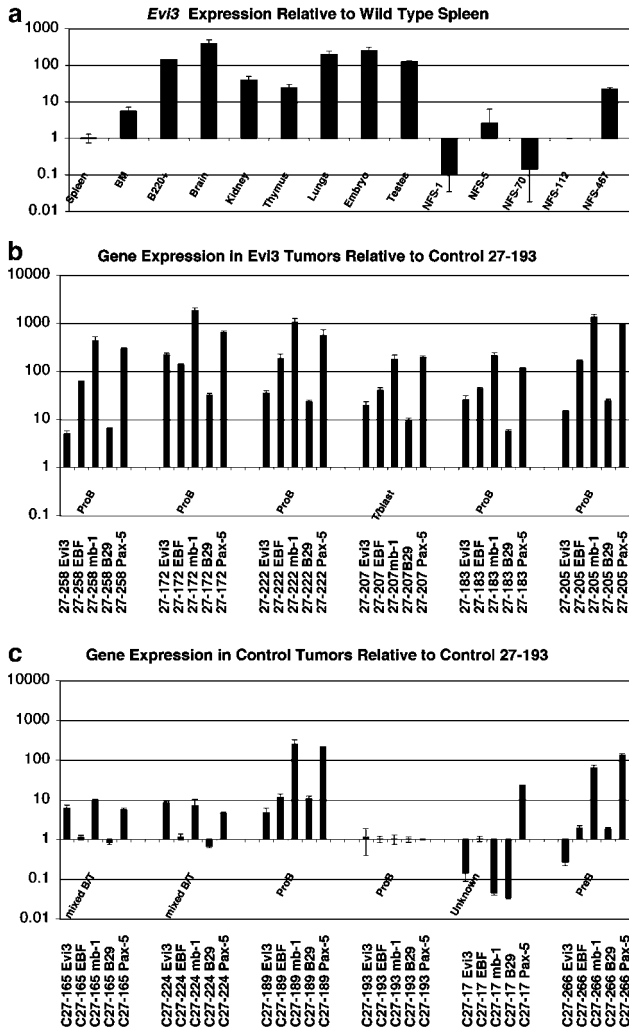


**Figure 2** Real-time PCR expression of *Evi3*, *EBF*, and *EBF* target genes in wild-type and tumor tissues. Panel a: The *Evi3* gene is highly expressed in wild-type brain, testes, lung, B220+ cells, and 12.5dpc embryos. Results are shown on a logarithmic scale and normalized to wild-type spleen. Panel b: Tumors with proviral insertions at *Evi3* show increased expression of *Evi3*. They also show increased expression of *EBF* and *EBF* target genes relative to control tumor C27-193. The tumor stage is shown. Results are shown on a logarithmic scale. Panel c: Tumors without viral insertions at *Evi3* have low levels of expression of *Evi3*, *EBF*, and *EBF* target genes relative to control tumor C27-193. When compared to tumors with *Evi3* insertions in panel b, these tumors do not show upregulation of *EBF* targets. The tumor stage is shown. Results are shown on a logarithmic scale. For all panels, error bars represent standard deviation

A16 into syngeneic mice. At 5 weeks after intraperitoneal injection of tumor cells, leukemias became visible in all mice as enlarged lymph nodes, and increased peripheral white blood cell counts. Southern blot analysis demonstrated that the reconstituted tumors maintained the viral insertions at *Evi3* in mice A235, A236, and A237, but not the control littermate A234, which was not injected with tumor cells (Table 2 and data not shown).

**Table 2** Molecular characteristics of reconstituted tumor A16

Mouse	<i>TCRβ1</i>	<i>TCR Jβ2</i>	<i>IgH</i>	<i>Igk</i>	<i>Evi3</i>
234	—	—	+	+	—
235	—	—	+	—	+
236	—	—	+	—	+
237	—	—	+	—	+

Animal number 234 is a spleen from a normal littermate, and therefore is not expected to contain *Evi3* rearrangements. It contains mature B-cells, and is therefore expected to have both *IgH* and *IgK* rearrangements. Animals 235, 236, and 237 were injected with frozen cells obtained from the original tumor A16. Note that all derivatives have the same molecular characteristics as the original tumor

Examination of reconstituted tumor cells by flow cytometry confirmed that they were of B-cell origin (Figure 3). The control littermate A234 lymph node exhibited a normal CD4/CD8 profile, while lymph nodes from tumor-bearing mice possessed virtually no CD4+ or CD8+ cells (Figure 3a). B220+ cells were found in low numbers and Thy-1+ cells found in high numbers in A234 control lymph nodes, whereas lymph nodes from mice A235, A236, and A237 contained almost exclusively B220+, Thy-1- cells (Figure 3b), demonstrating that the tumors are of B-cell origin.

We also assessed the tumor cells for a variety of B-cell surface markers to further localize the stage of developmental arrest (Figure 3c). The tumor cells were negative for a variety of temporally expressed B-cell markers, including the progenitor markers CD34 and CD117, and the immature marker sIgM (data not shown). However, in addition to B220, we identified three markers, CD19, CD38, and CD24, which are expressed in high densities on the surface of reconstituted tumor cells as compared to a wild-type littermate (Figure 3c). Both CD19 and CD38 are downstream of *EBF* (Lund *et al.*, 1996; Nutt *et al.*, 1997), providing further evidence that increased *Evi3* levels disrupts the normal *EBF* function.

To confirm that the increased CD19 levels were not specific to the A16 mouse we used to reconstitute the *Evi3* tumors, we analysed CD19 expression by Western blot in tumor tissue from five mice with *Evi3* viral insertions and two stage-matched control tumors (Figure 3d). All the tumors were Pro-B tumors (Table 1). We found that CD19 protein levels were elevated in the *Evi3* tumors as compared to controls (Figure 3d). Total protein was the same in all samples as demonstrated by *Gapdh* levels. Notably, the C27-189 tumor shows the highest CD19 protein expression of the control tumors. This same tumor also shows the highest RNA expression of *EBF* target genes by real-time PCR (Figure 2d), indicating that it is consistent to observe upregulation of several *EBF* targets in the same tumor. This tumor does not have viral insertions near *EBF* or any of the known *EBF* target genes, although the genes affected by the viral insertion in tumor C27-189 have not been characterized (<http://www.mouse-genome.bcm.tmc.edu/vstdata/>).

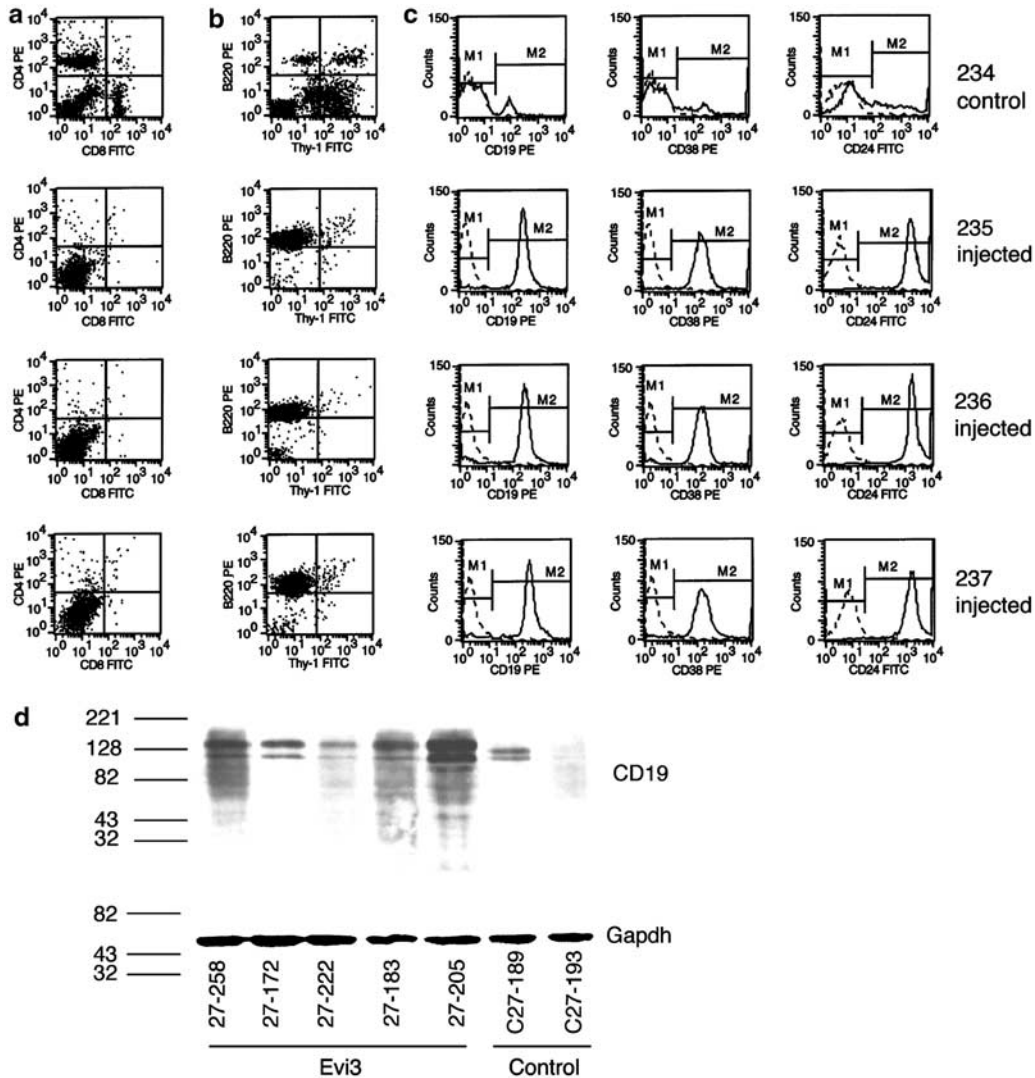


**Figure 3** Flow cytometry analysis of reconstituted tumors. Panel **a**: Surface marker expression of CD4 (vertical axis) and CD8 (horizontal axis). Panel **b**: Surface expression of B220 (vertical axis) and Thy1 (horizontal axis). Panel **c**: Surface expression of CD19 (column 1), CD38 (column 2), and CD24 (column 3). Animal 234 is a littermate control, animals 235, 236, and 237 were all injected with *Evi3* tumor cells. Cells from animals 235, 236, and 237 show increased levels of CD19, CD38, and CD24 as compared to the control animal 234. Panel **d**: Western blot analysis of CD19 expression (top) in *Evi3* tumors (lanes 1–5) and control tumors without *Evi3* viral insertions (lanes 6–7). The bottom blot shows Gapdh levels as a control for protein loading. Size markers in kilodaltons are shown to the left of the blots

The CD19 antibody used in these experiments recognizes different phosphorylation states of CD19. Interestingly, the bands observed in the control tumor, C27-189, show faster migration than the CD19 species in the *Evi3* tumors, indicating that, although CD19 protein is present in the controls, it is not highly phosphorylated. CD19 phosphorylation promotes B-cell receptor (BCR) signaling and leads ultimately to B-cell proliferation (Xu *et al.*, 2002); thus, the CD19 protein isoforms present in the *Evi3* tumors are consistent with increased BCR signaling due to EBF target activation.

#### *Evi3* modulation of EBF activity

To demonstrate that Evi3 can affect EBF transcriptional activation, we performed co-transfections of EBF

(Sigvardsson *et al.*, 1997) and a B29 promoter-luciferase construct (Akerblad *et al.*, 1999), which is a known target of EBF. We then co-transfected Evi3 to demonstrate that it could modulate the activation of the B29 reporter. When EBF and B29-luc are co-transfected into HEK293 cells, we see more than 10-fold upregulation of B29 activity compared to wells only transfected with the B29 reporter (Figure 4). Transfection of a vector control does not affect the levels of the B29-luc reporter. However, when Evi3 is added along with EBF, using the Evi3 IMAGE clone corresponding to the BC021376 sequence, we see a downregulation of B29 reporter activity to the baseline levels seen without EBF (Figure 4). We observed similar results when using the Evi3 image clone corresponding to the BI730849 sequence (data not shown). This is consistent

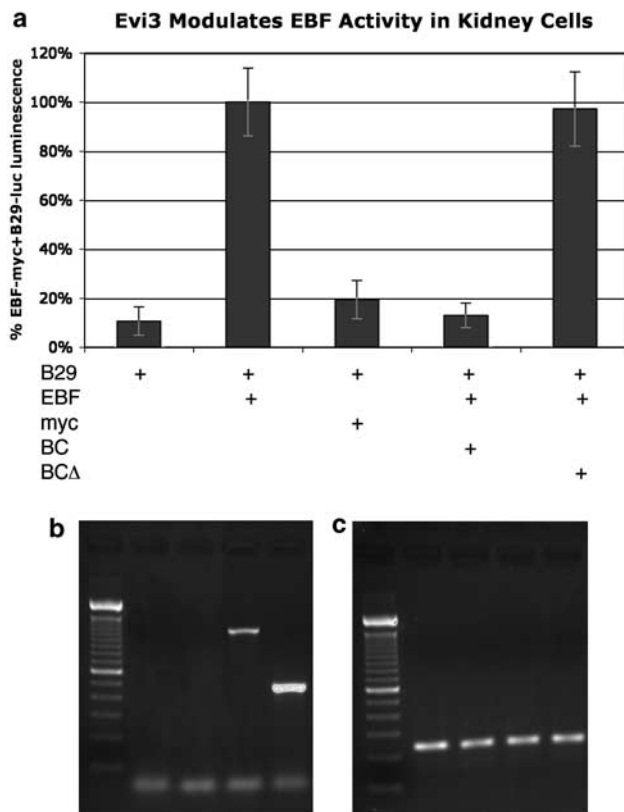


**Figure 4** Evi3 can modulate EBF activity in kidney cells. Panel a: Co-transfection of myc-EBF (EBF) and a B29-luciferase reporter (B29) shows upregulation of B29 expression (lane 2) as compared to B29 alone. Co-transfection of the myc-vector (myc) has no effect (lane 3). Co-transfection of myc-EBF, Evi3 (BC – clone BC021376), and B29 shows a reduction of B29 expression, almost to basal levels in the case of Evi3 clone BC021376 (lane 4). Co-transfection of EBF and Evi3 with a C-terminal truncation resulting in the removal of the final six zinc-fingers (BCΔ) shows no reduction in B29 levels (lane 6). Results are the averages of at least four co-transfections for each set of conditions. Error bars represent standard deviation. For each luciferase cell culture transfection experiment, normalized luminescence readings were divided by the average luminescence readings from cells co-transfected with myc-EBF and B29-luciferase. These values are expressed as a percentage of myc-EBF and B29-luciferase co-transfection. The plasmids added to each transfection are shown below the graph. Panel b: RT-PCR of half of the cells used in transfections for BC primers (span deletion region). Lane 1: 100 bp ladder, lane 2: B29-luciferase only, lane 3: B29-luciferase and EBF, lane 4: B29-luciferase, EBF, and BC, lane 5: B29-luciferase, EBF, and BCΔ. Note the smaller band amplified from the well transfected with the BCΔ construct. Panel c: RT-PCR for same samples as panel b with *Gapdh* primers, to confirm the presence of cDNA in all samples

with what has been reported for human Evi3 (Bond *et al.*, 2004).

It has been demonstrated that zinc-fingers 27–30 of the EBF<sub>FAZ</sub> protein interact with EBF (Tsai and Reed, 1998). We wanted to determine if the homologous zinc-fingers of Evi3 might modulate EBF transcriptional activity. We generated a deletion within the Evi3 EST BC021376 that eliminated the final six zinc-fingers of the

protein. The wild-type Evi3 protein is composed of 1311 amino acids. The protein in this new construct, called BCΔ, contains only the first 1013 amino acids of the Evi3 protein, followed by 57 unique amino acids caused by the disruption in reading frame from the deletion. The 57 amino-acid sequence was searched against the Blast nr protein database, as well as Swissprot and pdb, and was not found to contain any conserved domains or homology to any known proteins. Co-transfection of EBF, B29-luc, and BCΔ demonstrated no reduction in luciferase levels when compared to transfection of EBF and B29-luc, indicating that the C-terminal portion of the Evi3 protein is required for modulation of EBF activity (Figure 4a). The expression of Evi3 and the deletion construct BCΔ was confirmed by RT-PCR on cells from the transfection (Figure 4b and c). Additionally, this demonstrates that zinc-fingers homologous to the ones that mediate the protein–protein interaction between EBF<sub>FAZ</sub> and EBF are required for the interaction between Evi3 and EBF. This is the first demonstration of a functional interaction between a portion of the Evi3 protein and EBF.

## Discussion

*Evi3* has sequence similarity to EBF<sub>FAZ</sub>/Roaz, a multiple zinc-finger protein identified through its ability to interact with Olf-1/EBF (Tsai and Reed, 1997, 1998). EBF<sub>FAZ</sub> contains Krüppel zinc-fingers of the TFIIIA type, which can mediate protein–protein interactions as well as DNA–protein interactions (Tsai and Reed, 1998). The EBF<sub>FAZ</sub> protein interacts with SMADs in response to BMP2 signals through one group of zinc-fingers, while it interacts with EBF and SP-1 like GC-rich DNA sites through other zinc-fingers (Hata *et al.*, 2000). Due to the sequence similarity of *Evi3* and *EBF<sub>FAZ</sub>*, and to previous studies localizing Evi3 to the nucleus (Warming *et al.*, 2003), we propose that *Evi3* has a role in the development and/or differentiation of B-cells through the regulation of gene transcription (Figure 5). *EBF<sub>FAZ</sub>* has also been shown to interact with *Smads* to regulate mesoderm and neural development by activating the *Xenopus* genes *Xvent-2* (Hata *et al.*, 2000) and *Xretpos* (Shim *et al.*, 2002). Thus, it is possible that the *Evi3* gene also has additional roles in the regulation of normal embryonic development. We find high levels of *Evi3* expression in embryonic tissues, consistent with this theory. Additionally, we find expression of *Evi3* in nontumor tissues such as brain, suggesting that Evi3 may function in those tissues to regulate Smad activity.

Our expression analysis indicates that *Evi3* is upregulated in tumors due to viral insertions in the first intron of the *Evi3* gene, just upstream of the coding sequence. B-cell tumors without viral insertions at *Evi3* do not show overexpression of this gene, suggesting that the viral LTR drives the expression of *Evi3* in tumors (Warming *et al.*, 2003). *Evi3* has homology to EBF<sub>FAZ</sub>, a protein identified by its ability to interact with EBF. We demonstrate that EBF target genes have higher

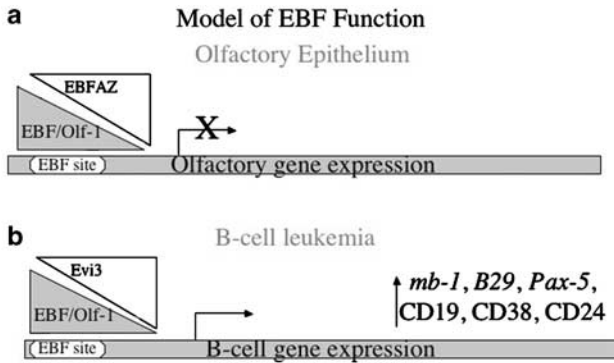


**Figure 5** Model of EBF activity. Panel a: Role of EBF in the olfactory epithelium. EBFAZ negatively regulates EBF activity to block the transcription of genes with EBF sites in their promoters. Panel b: Role of EBF in B-cell leukemia. Evi3 positively regulates EBF activity to promote the abnormal expression of B-cell target genes

expression in *Evi3* tumors as compared to tumors without viral insertions at *Evi3*. Taken together, these data suggest that overexpression of *Evi3* leads to the development of leukemia in mice with viral insertions at the *Evi3* locus.

Our results indicate that *Evi3* interacts with *EBF* during B-cell leukemogenesis. *EBF* is a B-cell transcription factor required for the initiation of B-lymphopoiesis in the bone marrow (Schebesta *et al.*, 2002). Along with the basic helix-loop-helix transcription factor *E2A*, *EBF* is required for the formation of B-cells from a common lymphoid progenitor cell (reviewed in Greenbaum and Zhuang, 2002). *EBF* expression induces the expression of B-cell-specific genes required for the activity of the B-cell receptor, including *mb-1* and *B29* (Schebesta *et al.*, 2002). The *mb-1* and *B29* genes encode the Ig- $\alpha$ /Ig- $\beta$  heterodimer, which associates with membrane-bound Ig molecules and contains the signaling activity of the B-cell receptor (Campbell *et al.*, 1991). The expression of *mb-1* and *B29* is upregulated in tumors with retroviral insertions at *Evi3* when compared to tumors without *Evi3* insertions, indicating that overexpression of *Evi3* leads to stimulation of *EBF* activity. This is in contrast to signaling in the olfactory epithelium, where EBFAZ association negatively regulates EBF function (Tsai and Reed, 1997).

In addition to the regulation of *mb-1* and *B29*, *EBF* also induces the expression of *Pax-5/BSAP* (O’Riordan and Grosschedl, 1999). Binding sites for EBF have been identified in the *Pax-5* promoter, and Pro-B-cells from mice that are lacking one copy of both *EBF* and the B-cell transcription factor *E2A* fail to express *Pax-5* (O’Riordan and Grosschedl, 1999). *Pax-5* is critical for the later development of B-cells, as *Pax-5*-deficient mice have a block in B-cell formation at the pre-B-cell stage, slightly later than the block seen in the *E2A* and *EBF* knockouts (reviewed in Maier and Hagman, 2002). Our results demonstrate that *Pax-5* expression is also upregulated in tumors with viral insertions at *Evi3*. A role for *Pax-5* in leukemogenesis is not unexpected, as

tumors with viral insertions at the *Pax-5* locus have also been identified (Suzuki *et al.*, 2002).

We found that the reconstituted *Evi3* tumors expressed higher levels of CD19 as compared to controls. Tumors from aged AKXD27 animals with *Evi3* insertions also demonstrated higher levels of CD19 protein than control tumors. The CD19/CD21 cell surface receptor complex transduces signals required for B-cell development and function (Hasegawa *et al.*, 2001). CD19 is a surface marker expressed throughout B-cell development, first appearing on pro-B cells (Zhou *et al.*, 1991). CD19-deficient mice have significantly fewer B cells in peripheral lymph nodes and spleen, impaired B-cell proliferation, and reduced serum Ig (Engel *et al.*, 1995). After BCR activation, CD19 phosphorylation is required to begin a cascade of signaling leading to B-cell proliferation (Xu *et al.*, 2002; Hase *et al.*, 2004). Interestingly, the CD19 protein present in *Evi3* tumors is more highly phosphorylated than the species found in controls, indicating that BCR signaling is activated in *Evi3* tumors.

Notably, CD19 is regulated by *EBF* in the human (Gisler *et al.*, 1999). While it has not been shown to be under direct EBF control in the mouse, it is likely that EBF promotes mouse CD19 expression in B-cells, through regulation of *Pax-5/BSAP* signaling. *Pax-5* is a target of EBF, and there are EBF-binding sites in the *Pax-5* promoter (O’Riordan and Grosschedl, 1999). Additionally, *Pax-5* has been demonstrated to bind to sequences in the *CD19* promoter (Nutt *et al.*, 1997). *Pax-5*-deficient mice lack *CD19* expression (Nutt *et al.*, 1997). There is further evidence that EBF and *Pax-5* act in concert to regulate B-cell development. The EBF target gene, *mb-1*, is also a target of *Pax-5* (Nutt *et al.*, 1998). Pre-B-cells isolated from *Pax-5*-deficient mice lack *mb-1* expression (Nutt *et al.*, 1998). Promoter analysis demonstrated that EBF, *E2A*, and *Pax-5* regulate *mb-1* expression during B-cell development, with EBF and *E2A* controlling expression at the pre-B-cell stage, and *Pax-5* promoting *mb-1* expression in later stages of B-cell development (Sigvardsson *et al.*, 2002). Thus, proper EBF function is required for B-cell development and function. We demonstrate here that *Evi3* overexpression disrupts this pathway in tumors with *Evi3* viral insertions.

CD38 has been implicated as a multi-role surface molecule differentially expressed by immature and activated cells of a variety of lineages. Interestingly, CD38 signaling requires expression of a functional B-cell receptor complex (Lund *et al.*, 1996, 1999; Donis-Hernandez *et al.*, 2001). The B-cell receptor is encoded by the *mb-1* and *B29* genes, which are known targets of EBF. Thus, CD38 is likely also a downstream target of EBF. The upregulation of CD38 in reconstituted *Evi3* tumors, similar to the upregulation of *mb-1*, *B29*, and CD19, is consistent with this theory.

We also demonstrate that *Evi3* can modulate EBF transcriptional activity. In HEK293 cells, we observe that co-transfection of *Evi3* and *EBF* decreases the expression of *B29*, an EBF-target gene. This is consistent with results for co-transfection of the human

homolog of *Evi3* (Bond *et al.*, 2004). We have also determined that the C-terminal region of *Evi3* is required for modulation of EBF activity. Interestingly, in our tumor samples, we see upregulation of EBF targets when *Evi3* expression increases. Although HEK293 cells do express *Evi3* (Bond *et al.*, 2004), it is possible that in kidney cells there are other factors that cause downregulation of EBF targets, contrary to the results shown in B-leukemia cells. In wild-type kidney cells, we do detect *Evi3* expression at a level higher than wild-type spleen, indicating that *Evi3* must have some function in this tissue unrelated to lymphoid differentiation. Thus, perhaps in nonleukemic tissues, *Evi3* expression leads to a downregulation of EBF target genes, while in leukemogenic cells *Evi3* expression leads to upregulation of EBF targets.

*Evi3* transcripts have been detected in several lymphomatous pro-B and pre-B lines, but are missing in an immature B-cell line (Justice *et al.*, 1994), suggesting that *Evi3* is differentially regulated in B-cell development. It is likely that *Evi3* controls temporal events in early B-cell lymphopoiesis, which regulate the *EBF* differentiation pathway, and its abnormal expression may alter normal developmental processes to lead to the development of leukemias. Several downstream targets of *EBF* activity are upregulated in *Evi3* tumors, indicating that *Evi3* can modulate EBF transcriptional activity. While mice that lack functional EBF pathway members fail to produce B-cells (reviewed in Greenbaum and Zhuang, 2002; Maier and Hagman, 2002), this study suggests that activation of EBF targets through increased *Evi3* expression can cause B-cell leukemia.

## Materials and methods

### Mice

AKXD-27 recombinant inbred mice have been described elsewhere (Mucenski *et al.*, 1986; Justice *et al.*, 1994). Mice were aged and sacrificed as tumors became apparent. Mice failing to show disease manifestations by 14 months were killed and examined for tumors.

### Tumor processing

Tumors for DNA were removed from mice and snap-frozen in liquid nitrogen. Single-cell suspensions of tumors were made by gently disrupting tumors in Hank's balanced salt solution (HBSS; Life Technologies, Bethesda, MD, USA; Schountz *et al.*, 1996). Cells were resuspended in tumor medium at  $10^6$  cells/ml, then tissue culture grade DMSO (Sigma) was added to 10% v/v. Cells were stored frozen in liquid nitrogen.

### Southern blot analysis

High molecular weight DNA was prepared from snap-frozen tumors described above (Mucenski *et al.*, 1986). Restriction enzyme digestion to detect rearrangements at the IgH (*EcoRI*), Ig $\kappa$  (*BglII*), TCR  $\beta$ 1 (*PvuII*),  $\beta$ 2 (*HindIII*), and *Evi3* (*XbaI*) loci and Southern hybridization have been detailed elsewhere (Gilbert *et al.*, 1993; Justice *et al.*, 1994). Probes for IgH, Ig $\kappa$ , TCR  $\beta$ 1, and  $\beta$ 2 have been described elsewhere (Kronenberg *et al.*, 1985; Mucenski *et al.*, 1986). The probe for *Evi3* was

prepared from a 1 kb *KpnI* genomic fragment cloned into pBluescript KS<sup>+</sup> (Justice *et al.*, 1994). Radiolabeled probes were synthesized with a Prime-It™ kit according to the manufacturer's directions (Stratagene, La Jolla, CA, USA).

### EST clone sequencing

EST clones were purchased from Research Genetics (Huntsville, AL, USA). Cycle sequencing was performed with the ABI Big Dye sequencing kit according to the manufacturer's instructions using standard sp6 and T7 oligo primers. Sequencing reactions were analysed in the Baylor College of Medicine Department of Molecular and Human Genetics Sequencing Core. Analysis of DNA sequence was performed using Sequencher 4.1 software (Gene Codes Corp., Ann Arbor, MI, USA).

### Protein sequence analysis

*Evi3* and EBFAZ protein sequence alignments were performed using clustalw (<http://www.ebi.ac.uk/clustalw>). Protein sequences were also analysed with Interpro scan to identify conserved domains (<http://www.ebi.ac.uk/interpro/scan.html>).

### Real-time PCR analysis

**RNA extraction** Total RNA was extracted from the tissues using RNA STAT-60 total RNA/mRNA isolation reagent according to the manufacturer's instructions (Tel-Test, Inc., Friendswood, TX, USA). The RNA pellet was dissolved in 40  $\mu$ l of DEPC-water and treated with DNase I, amplification grade (Invitrogen) for 30 min at 37°C.

**Reverse transcription** ABI Reverse Transcription kits were used for generating cDNA. In all, 2  $\mu$ g of RNA was added to a reaction containing 1  $\times$  RT buffer, 5.5 mM MgCl<sub>2</sub>, 500  $\mu$ M per dNTP, 2.5  $\mu$ M random hexamers, 0.4 U/ $\mu$ l RNase inhibitor, and 3.125 U/ $\mu$ l Multiscribe Reverse Transcriptase, for a total reaction volume of 100  $\mu$ l. The RT thermal cycling parameters used for samples with random hexamers were 25°C for 10 min, 37°C for 60 min, and 95°C for 5 min.

**Real-time quantitative PCR** All primers were optimized on the ABI 7000 SDS using the SYBR Green dye. All samples for quantitative PCR were run in triplicates. In all, 1  $\mu$ l of the cDNA was added to the optimal mix of the forward and reverse primers and 1  $\times$  SYBR Green PCR master mix to get a final reaction volume of 50  $\mu$ l. The following thermal cycling parameters were used for quantitative PCR using ABI 7000 SDS: 95°C for 10 min, 40 cycles of 95°C for 15 s, and 60°C for 1 min.

**Data analysis** Real-time PCR was analysed using relative expression levels (Bieche *et al.*, 2001). Expression of the genes was compared to both an endogenous RNA control, *18S* RNA, and to levels in wild-type spleen as a tissue control for the tumors, similar to the method described by Bieche *et al* (2001).

### PCR primer sequences:

*Mb-1* #1: ttcttgcatcagcctgtttgg  
*Mb-1* #2: aagttcaccgtcaggatggt  
*B29* #1: agacctctcatcatcctcttc  
*B29* #2: cagccttgccgtcatcctt  
*Evi3* #1: gcgacagcgcagtccaa  
*Evi3* #2: gatctcggtttcgcttgctt  
*18S* #1: gtaacccttggaacccatt

18S #2: ccatccaatcggtagtagcg  
 EBF #1: gctcctctggcactcttctcctt  
 EBF #2: gcgaaagcactcttctgtttca  
 Pax-5 #1: cgacaccaacaacgcaaga  
 Pax-5 #2: ccggaagtgagtgccatt

#### Reconstitution of tumors

Frozen single tumor-cell suspensions were quick-thawed at 37°C. Cells were washed 2 × with tumor medium, then 3 × in sterile PBS. Cells were adjusted to 5 × 10<sup>7</sup>/ml and 200 μl was injected intraperitoneally into 12-week-old sex-matched AKXD-27 mice. Tumors appeared in 5 weeks and mice were processed as described above.

#### Flow cytometry

Cells were washed and adjusted to 2 × 10<sup>6</sup>/ml in wash buffer (5% FBS-PBS), and 100 μl pipetted into the wells of V-bottom 96-well microtiter plates (Nunc). Plates were centrifuged to pellet cells, supernatants decanted and cells resuspended by gentle vortexing. Wash buffer containing antibody conjugates (Pharmingen) was added to the wells, followed by incubation on ice for 45 min. Antibodies used were to CD4 (RM4-4), CD8α (53-6.7), CD19 (1D3), CD24 (M1/69), CD34 (RAM34/49E8), CD38 (90), CD117 (2B8), B220 (cat #553086), and Thy1 (cat #553013). Cells were washed twice, then fixed in 1% paraformaldehyde, and 10000 events collected with a FACStar flow cytometer (Becton-Dickinson) as described previously (Schountz *et al.*, 1996).

#### Western blot

Tumor tissue was homogenized in RIPA protein lysis buffer. Membrane blocking and antibody incubations were performed according to the manufacturer's protocol for anti-CD19 (1 : 500 dilution, cat #3574, Cell Signaling Technology), and anti-Gapdh (1 : 2500 dilution, clone 6C5, Advanced Immunochemical). Protein expression was visualized using the ECL Western Blotting Analysis System (RPN-2108, Amersham Biosciences) according to the manufacturer's instructions.

#### References

Akerblad P, Rosberg M, Leanderson T and Sigvardsson M. (1999). *Mol. Cell. Biol.*, **19**, 392–401.  
 Bieche I, Parfait B, Laurendeau I, Girault I, Vidaud M and Lidereau R. (2001). *Oncogene*, **20**, 8109–8115.  
 Bond HM, Mesuraca M, Carbone E, Bonelli P, Agosti V, Amodio N, De Rosa G, Di Nicola M, Gianni A, Moore MS, Hata A, Grieco M, Morrone G and Venuta S. (2004). *Blood*, **103**, 2062–2070.  
 Campbell KS, Hager EJ, Friedrich RJ and Cambier JC. (1991). *Proc. Natl. Acad. Sci. USA*, **88**, 3982–3986.  
 Donis-Hernandez FR, Parkhouse ME and Santos-Argumedo L. (2001). *Eur. J. Immunol.*, **31**, 1261–1267.  
 Engel P, Zhou L, Ord D, Sato S, Koller B and Tedder T. (1995). *Immunity*, **3**, 39–50.  
 Gilbert D, Neumann P, Taylor B, Jenkins N and Copeland N. (1993). *J. Virol.*, **67**, 2083–2090.  
 Gisler R, Akerblad P and Sigvardsson M. (1999). *Mol. Immunol.*, **36**, 1067–1077.  
 Gisler R, Jacobsen SE and Sigvardsson M. (2000). *Blood*, **96**, 1457–1464.

#### Cell culture and transfection

HEK293 cells were cultured in RPMI 1640 medium with L-glutamine (Invitrogen), 50 mM HEPES, and 10% FBS. Transfections were carried out using 100 ng of pMDEBF (myc-EBF), pMDCDNA (myc tag vector), pBC (Evi3 clone #BC021376), pBCΔ (Evi3 clone #BC021376 with a deletion between bases 3087 and 3796), and pB29-luc (B29 reporter) plasmids with 20 ng of pRLCMV for a transfection efficiency control and 1 μl FuGene (roche) lipfection reagent in a six-well plate format. Luciferase assays were performed using the Dual Luciferase Assay Kit (Promega) with normalization to renilla luciferase to control for transfection efficiency. All transfections were repeated at least four times. To confirm that the BC and BCΔ constructs were expressed in the transfections, half of the cells were removed from each well and used to prepare RNA (Wizard kit, Promega) and then reverse transcribed into cDNA (ABI reverse transcription kit). RT-PCR was performed with primers that span the deleted region of the Evi3 gene (BC for: tggataccggaactgtcgta, BC rev: ggagtctgtctatctgtgtct). For each luciferase cell culture transfection experiment, normalized luminescence readings were divided by the average luminescence readings from cells co-transfected with myc-EBF and B29-luciferase. These values are expressed as a percentage of myc-EBF and B29-luciferase co-transfection. The BCΔ construct was generated by digesting BC021376 with *Bsu36I* and *BstBI*. This removed an approximately 700 bp fragment from the construct. The ends of the construct were filled in, and a blunt ligation was performed. The correct ligation of the ends was verified by sequencing (primer sequence: tggataccggaactgtcgta). Plasmids were purified for transfection using a midi-prep kit (Qiagen).

#### Acknowledgements

We thank Dr Mikael Sigvardsson for the myc-EBF, myc vector, and B29-luciferase constructs. We thank Toni L Jago, Shamsha Damani, Antoine Perchellet, and Mary E Stech for superb technical assistance. We thank D Popp for technical assistance with FACS analysis and G Hansen for assistance in tumor processing. We thank Dr Yuan Zhuang for critical reading of the manuscript. Tumor insertion site sequences and chromosomal location can be viewed at: <http://www.mouse-genome.bcm.tmc.edu/vstdata/>. This work was supported by PHS grants R01 CA63229 to MJJ and F32 HD42436 to KEH.

Greenbaum S and Zhuang Y. (2002). *Semin. Immunol.*, **14**, 405–414.  
 Hagman J, Belanger C, Travis A, Turck CW and Grosschedl R. (1993). *Genes Dev.*, **7**, 760–773.  
 Hansen GM, Skapura D and Justice MJ. (2000). *Genome Res.*, **10**, 237–243.  
 Hase H, Kanno Y, Kojima M, Hasegawa K, Sakurai D, Kojima H, Tsuchiya N, Tokunaga K, Masawa N, Azuma M, Okumura K and Kobata T. (2004). *Blood*, **103**, 2257–2265.  
 Hasegawa M, Fujimoto M, Poe JC, Steeber DA and Tedder TF. (2001). *J. Immunol.*, **167**, 3190–3200.  
 Hata A, Seoane J, Lagna G, Montalvo E, Hemmati-Brivanlou A and Massague J. (2000). *Cell*, **100**, 229–240.  
 Kronenberg M, Goverman J, Haars R, Malissen M, Kraig E, Phillips L, Delovitch T, Suci-Foca N and Hood L. (1985). *Nature*, **313**, 647–653.  
 Justice MJ, Morse HR, Jenkins N and Copeland N. (1994). *J. Virol.*, **68**, 1293–1300.

- Lund FE, Muller-Steffner HM, Yu N, Stout CD, Schuber F and Howard MC. (1999). *J. Immunol.*, **162**, 2693–2702.
- Lund FE, Yu N, Kim K-M, Reth M and Howard MC. (1996). *J. Immunol.*, **157**, 1455–1467.
- Maier H and Hagman J. (2002). *Semin. Immunol.*, **14**, 4154–4422.
- Mucenski M, Bedigian H, Shull M, Copeland N and Jenkins N. (1988). *J. Virol.*, **62**, 839–846.
- Mucenski M, Gilbert D, Taylor B, Jenkins N and Copeland N. (1987). *Oncogene Res.*, **2**, 33–48.
- Mucenski M, Taylor B, Jenkins N and Copeland N. (1986). *Mol. Cell. Biol.*, **6**, 4236–4243.
- Nutt SL, Morrison AM, Dörfler P, Rolink A and Busslinger M. (1998). *EMBO J.*, **17**, 2319–2333.
- Nutt SL, Urbanek P, Rolink A and Busslinger M. (1997). *Genes Dev.*, **11**, 476–491.
- O’Riordan M and Grosschedl R. (1999). *Immunity*, **11**, 21–31.
- Schebesta M, Heavey B and Busslinger M. (2002). *Curr. Opin. Immunol.*, **14**, 216–223.
- Schountz T, Kasselmann J, Martinson F, Brown L and Murray J. (1996). *J. Immunol.*, **157**, 3893–3901.
- Shim S, Bae N and Han JK. (2002). *Nucleic Acids Res.*, **30**, 3107–3117.
- Sigvardsson M, Clark DR, Fitzsimmons D, Doyle M, Akerblad P, Breslin T, Bilke S, Li R, Yeaman C, Zhang G and Hagman J. (2002). *Mol. Cell. Biol.*, **22**, 8539–8551.
- Sigvardsson M, O’Riordan M and Grosschedl R. (1997). *Immunity*, **7**, 25–36.
- Smith EMK, Gisler R and Sigvardsson M. (2002). *J. Immunol.*, **169**, 261–270.
- Suzuki T, Shen H, Akagi K, Morse HC, Malley JD, Naiman DQ, Jenkins NA and Copeland NG. (2002). *Nat. Genet.*, **32**, 166–174.
- Tsai RY and Reed RR. (1997). *J. Neurosci.*, **17**, 4159–4169.
- Tsai RY and Reed RR. (1998). *Mol. Cell. Biol.*, **18**, 6447–6456.
- Wang SS, Tsai RY and Reed RR. (1997). *J. Neurosci.*, **17**, 4149–4158.
- Warming S, Liu P, Suzuki T, Akagi K, Lindtner S, Pavlakis GN, Jenkins NA and Copeland NG. (2003). *Blood*, **101**, 1934–1940.
- Xu Y, Beavitt S-JE, Harder KW, Hibbs ML and Tarlington DM. (2002). *J. Immunol.*, **169**, 6910–6918.
- Zhou L, Ord D, Hughes A and Tedder T. (1991). *J. Immunol.*, **147**, 1424–1432.